Saudi Pharmaceutical Journal (2016) **24**, 74–81

King Saud University

Saudi Pharmaceutical Journal

www.ksu.edu.sa
www.sciencedirect.com

ORIGINAL ARTICLE

Pravastatin chitosan nanogels-loaded erythrocytes as a new delivery strategy for targeting liver cancer

Gamaleldin I. Harisa [a,c,*], Mohamed M. Badran [b,d], Saeed A. AlQahtani [a,b], Fars K. Alanazi [a,b], Sabry M. Attia [e,f]

[a] *Kayyali Chair for Pharmaceutical Industry, Department of Pharmaceutics, College of Pharmacy, King Saud University, P.O. Box 2457, Riyadh 11451, Saudi Arabia*
[b] *Department of Pharmaceutics, College of Pharmacy, King Saud University, P.O. Box 2457, Riyadh 11451, Saudi Arabia*
[c] *Department of Biochemistry, College of Pharmacy, Al-Azhar University, Cairo, Egypt*
[d] *Department of Pharmaceutics, College of Pharmacy, Al-Azhar University Cairo, Egypt*
[e] *Department of Pharmacology and Toxicology, College of Pharmacy, King Saud University, Riyadh, Saudi Arabia*
[f] *Department of Pharmacology and Toxicology, College of Pharmacy, Al-Azhar University, Cairo, Egypt*

Received 9 March 2015; accepted 16 March 2015
Available online 21 March 2015

KEYWORDS

Erythrocytes;
Hypotonic preswelling;
Chitosan nanogels;
Pravastatin;
Liver targeting

Abstract Chitosan nanogels (CNG) are developed as one of the most promising carriers for cancer targeting. However, these carriers are rapidly eliminated from circulation by reticuloendothelial system (RES), which limits their application. Therefore, erythrocytes (ER) loaded CNG as multifunctional carrier may overcome the massive elimination of nanocarriers by RES. In this study, erythrocytes loaded pravastatin–chitosan nanogels (PR–CNG–ER) were utilized as a novel drug carrier to target liver cancer. Thus, PR–CNG formula was developed in nanosize, with good entrapment efficiency, drug loading and sustained release over 48 h. Then, PR–CNG loaded into ER were prepared by hypotonic preswelling technique. The resulting PR–CNG–ER showed 36.85% of entrapment efficiency, 66.82% of cell recovery and release consistent to that of hemoglobin over 48 h. Moreover, PR–CNG–ER exhibited negative zeta potential, increasing of hemolysis percent, marked phosphatidylserine exposure and stomatocytes shape compared to control unloaded

* Corresponding author at: Department of Pharmaceutics, College of Pharmacy, King Saud University, P.O. Box 2457, Riyadh 11451, Saudi Arabia. Tel.: +966 546269544; fax: +966 (11) 4676295.
E-mail address: gamal.harisa@yahoo.com (G.I. Harisa).
Peer review under responsibility of King Saud University.

Production and hosting by Elsevier

http://dx.doi.org/10.1016/j.jsps.2015.03.024

erythrocytes. PR–CNG–ER reduced cells viability of HepG2 cells line by 28% compared to unloaded erythrocytes (UER). These results concluded that PR–CNG–ER are promising drug carriers to target liver cancer.

1. Introduction

Nanocarriers could secretively target tumor tissues through enhanced permeability and retention (EPR) effect. Therefore, they increased therapeutic efficacy, and decreased side effects of anticancer agents (Upreti et al., 2013). The application of nanogels (NG) in the field of drug delivery received great attention in the last years (Hamidi et al., 2008). They are smart delivery systems, biodegradable, biocompatible, and absorption enhancer (Bhattarai et al., 2010). Chitosan widely was used in nanocarriers technology for delivery of anticancer; moreover, it has hypocholesterolemic, anticancer effects and many other beneficial effects (Xia et al., 2011; Keawchaoon and Yoksan, 2011). However, administration of nanocarriers may result in hypersensitivity reactions and rapid clearance by macrophages (Reijnders, 2006; Fan et al., 2012).

Chitosan nanogels (CNG) and erythrocytes that in combination complement each other are desirable approaches as multifunctional drug carrier with immuno-invasive properties was reported by Fan et al. (2012). In such cases nanocarriers coated with erythrocytes represent a major advance in drug delivery technology (Hu et al., 2011; Fang et al., 2012). This overcomes immune activation properties, and massive clearance of nanocarriers by macrophages (Hu et al., 2011). Several studies reported that CNG are promising drug nanocarriers and can be loaded into erythrocytes (Hamidi et al., 2011; Fan et al., 2012). As drug vehicle erythrocytes (ER) are biocompatible, biodegradable, and have long life span, several methods for drug loading were developed (Kostić et al., 2014). Drug loaded erythrocytes can effectively target reticuloendothelial system (RES) (Yew et al., 2013). The loaded erythrocytes can be extravasated only in the opening of hepatic sinuses. However, nanoparticles extravasate in tumor tissues by EPR effect (Muzykantov, 2010).

Abnormal cholesterol homeostasis was observed and several types of cancers, cholesterol biosynthesis and uptake increased; however, cholesterol efflux decreased (Smith and Land, 2012; Jiang et al., 2007; Menter et al., 2011). Therefore, targeting of cholesterol biosynthesis is considered as a novel approach for the treatment of hepatocellular carcinoma (HCC) (Zhang and Du, 2012). Statins block 3-hydroxy-3-methylglutaryl coenzyme A (HMG-CoA) reductase pathway in the liver (Smith and Land, 2012; Montori et al., 2014). Several studies demonstrated that statins protect against liver cancer (Smith and Land, 2012). Particularly, pravastatin (PR) has the ability to reduce proliferation of HCC lines and reduce the risk of liver cancer (Graf et al., 2008). Further studies are required to address this issue.

Therefore, the aim of this study was to prepare and characterize erythrocytes loaded pravastatin–chitosan nanogels (PR–CNG–ER) as a novel drug carrier to target liver cancer. To our knowledge, this delivery system of PR was described for the first time. To achieve this goal, PR–CNG were prepared and characterized in terms of physic-chemical properties, entrapment efficiency, drug loading and in vitro release study. Then, the prepared PR–CNG were loaded into ER by hypotonic preswelling method. Thus, the prepared PR–CNG–ER were characterized for their drug encapsulation, drug loading and drug release. Finally, the PR–CNG–ER were investigated as a new antitumor strategy to target liver cancer using HepG2 cells as an in vitro model of HCC.

2. Materials and methods

2.1. Materials

Pravastatin was purchased from Riyadh Pharma, Riyadh, Saudi Arabia. Sodium tripolyphosphate (TPP) and glacial acetic acid were obtained from BDH, UK. Low molecular weight chitosan (70 kDa with the degree of deacetylation 75–85%), Assay kit MTT, HepG2 cell line human and dimethyl sulfoxide (DMSO) were obtained from Sigma–Aldrich (St. Louis, MO, USA). All other chemicals used were of reagent grade.

2.2. Preparation and characterization of PR–CNG

The dispersion of CNG was prepared following an ionic gelation method. The CNG system investigated here composed of chitosan (3% w/w) and TPP (1% w/w). Briefly, TPP solution was added dropwise to 0.5 w/v of acidic solution of chitosan under vigorous magnetic stirring at room temperature. The nanogel was formed spontaneously as a result of interaction between the negative groups of TPP and the positively charged amino groups of chitosan. The final CNG were probe-sonicated for 3 min in order to break any aggregations and reduce particle size. The particle size, polydispersity index (PDI) and zeta potential of particles were measured by Zetasizer based on the dynamic light scattering (DLS) technique. The entrapment efficiency and drug loading were calculated after centrifugation at 16,000 rpm for a period of 30 min and the amount of PR in supernatants was determined. The CSN were freeze-dried and stored at 5 °C. The morphological characteristics of nanoparticles were investigated by Scanning electron microscope (SEM). Structural features of CNG were estimated by Fourier transform infrared (FTIR) and X-ray diffraction (Hamidi et al., 2011).

2.3. Preparation and characterization of PR–CNG–ER

2.3.1. Preparation of erythrocyte suspension

The blood specimens were collected in heparinized tubes from apparently healthy donors not suffered from acute and chronic diseases. Informed consent was obtained from the donor. The experimental protocol was done according to our institutional

guidelines. The collected specimens were centrifuged for 10 min at 3000 rpm. The plasma and the puffy coat were removed by aspiration. Packed erythrocytes were washed three times with phosphate buffered saline (PBS). The hematocrit was adjusted to 45% using PBS (Hamidi et al., 2007).

2.3.2. Loading of erythrocytes with PR–CNG

A modified hypotonic preswelling was used for loading of PR–CNG and free PR into human erythrocytes. Three ml of washed packed erythrocytes was transferred gently to test tube. Twelve ml of hypotonic solution (0.6% NaCl) was added. The resulting cell suspension was mixed several times by gentle inversion. The swollen cells produced were separated by centrifugation at 3000 rpm for 5 min and the supernatant was discarded. Eight hundred µl of PR–CNG (5 mg/ml) in aqueous solution was added gently to cell suspension, and the resulting mixture was inverted gently several times. This step was repeated three times to achieve lysis point of the cells, then incubated at 0 °C for 10 min, and resealed by the addition of 600 µl of hypertonic solution (KCl 1.5 M). Finally, the resulting mixture was incubated at 37 °C for 30 min. Resultant PR–CNG–ER were washed three times with PBS. PR loaded erythrocytes (PR-ER), PR–CNG-loaded erythrocytes and sham-encapsulated erythrocytes (SH-ER) were prepared as described except for replacing PR–CNG with PR, plane CNG, and distilled water respectively. The loading parameters were determined as described by Hamidi et al., (2007).

2.3.3. Hematological indices

The mean corpuscular volume (MCV), mean corpuscular hemoglobin (MCH); mean corpuscular hemoglobin content (MCHC) of unloaded erythrocytes (UER) and loaded erythrocytes were determined using Coulter® LH 780 hematology analyzer.

2.3.4. Zeta potential

Zeta potential of CS solution, CNG, PR–CNG, PR-ER and PR–CNG–ER and control erythrocytes were determined using Zetasizer Nano ZS (Malvern Instruments, UK).

2.3.5. Hemolysis studies

This test was performed to assess the behavior of erythrocyte membranes toward osmotic pressure changes in their surrounding media. Twenty-five µl of control, SH-ER, PR–CNG, PR–CNG–ER and PR-ER was mixed with 2.5 ml of NaCl aqueous solutions (0.4% NaCl solution). After 30 min the mixtures were centrifuged at 3000 rpm for 10 min, and the absorbance of the supernatants was determined spectrophotometrically at 540 nm. The released hemoglobin was expressed as percentage absorbance of each sample compared to the released hemoglobin from complete hemolyzed sample (Kraus et al., 1997).

2.3.6. Detection of phosphatidylserine exposure

Exposure of the phosphatidylserine (PS) on the outer leaflet of the erythrocytes membrane bilayer was quantified by Annexin V binding test according to manufacturer procedures (BD Pharmingen PE Annexin V Apoptosis Detection Kit). Briefly, each type of erythrocytes was resuspended in ice-cold Annexin V Binding Buffer (10 mM Hepes (pH 7.4), 140 mM NaCl, and 2.5 mM CaCl2), kept on ice before the Annexin V-FITC solution was added. Then, tubes were incubated for 15 min in the dark place. The samples were analyzed within 30 min using flow cytometry. The cells are having FITC fluorescence higher than cutoff value of non-specific fluorescence declared as Annexin V positive. The percentage of positive cells was expressed as the ratio of labeled to total cell number.

2.3.7. Scanning electron microscopy (SEM)

A JEOL JSM-6380 LA scanning electron microscope (Jeol Ltd., Tokyo, Japan) was used to evaluate erythrocytes morphological differences between control, SH-ER, PR–CNG–ER, and PR-ER. The cells were fixed in buffered glutaraldehyde, rinsed 3 times for 5 min in phosphate buffer and post-fixed in osmium tetroxide for 1 h. Afterward, samples were rinsed with distilled water and dehydrated using a graded ethanol series: 25%, 50%, 75%, and 100% 10 min for each. Finally, samples were rinsed in water, removed, mounted and then viewed using SEM (Harisa et al., 2012).

2.3.8. Pravastatin and hemoglobin release

To exploit the release kinetics of PR–CNG–ER, and hemoglobin from carrier erythrocytes, 0.5 ml of packed PR–CNG–ER was diluted to 5 ml using ringer solution. The suspension was mixed thoroughly by several gentle inversions and, then, placed in Shaking Water Bath: SW22 (Julabo Labortechnik GmbH, Seelbach, Germany) set at 150 rpm and 37 °C. After 0.25, 0.5, 1, 2, 4, 6, 8, 12, 24 and 48 h incubation, one of the aliquots was harvested, 200 µl of the supernatants were extracted by 500 µl of methanol through vortexing and centrifuging at 13,000 rpm for 30 min, then, injected directly to chromatograph for PR assay. In addition, the absorbance of another 200 µl portion of the supernatant diluted with 1 ml of PBS was determined at 540 nm using a UV/visible spectrophotometer to monitor the hemoglobin release. The initial volume of release medium was maintained by refilling 200 µl of the ringer solution after each withdrawal. These experiments were carried out in triplicate (Hamidi et al., 2007; Hamidi et al., 2011).

2.3.9. UPLC assay of PR

PR was analyzed according to our previously described ultra-performance liquid chromatography (UPLC) method. The mobile phase contained a mixture of 0.25% formic acid in distilled water and acetonitrile (65:35, v/v) for UV detection (Abdel-Hamid et al., 2012).

2.4. Cytotoxicity study

HepG2 cells were used to study the effect of loaded (PR–CNG–ER) and unloaded erythrocytes (control) on cell viability. The 3-(4,5-dimethylthiazol-2-yl)-2,5-diphenyl-tetrazolium bromide (MTT) assay was used in the present study. This colorimetric assay is based on conversion of yellow tetrazolium bromide (MTT) to the purple formazan derivatives by mitochondrial succinate dehydrogenase in viable cells. HepG2 cells were seeded at a density of 5000 cells/ml, and incubated at 37 °C and 5% CO_2 atmosphere in a culture plate. HepG2 cell line was incubated with unloaded erythrocytes

(control), pravastatin-loaded erythrocytes (PR-ER), CNG-loaded erythrocytes (CNG–ER) or PR–CNG–ER. After 72 h incubation time, the medium was removed, and the wells were washed with phosphate buffer saline. Ten μl of MTT solution was added to each well and incubated for 3 h. Then, the absorbance was measured at 570 nm in a microplate reader. The cell viability was calculated by the following equation:

$$\text{Cell viability } \% = \frac{\text{Absorbance sample}}{\text{Absorbance control}} \times 100$$

2.5. Statistical analysis

Data are expressed as mean ± standard deviation (S.D) for the groups. Data analysis was evaluated by one-way ANOVA (analysis of variance) followed by Tukey–Kramer test for multiple comparisons. Data analysis was performed using GraphPad InStat software, Version 4 (GraphPad, ISI Software Inc., La Jolla, CA, USA). A 0.05 level of probability was used as the criterion for significance.

3. Result and discussion

In the present study, unloaded and PR-loaded CNG were characterized by DLS and drug loading. The unloaded showed a unimodal size distribution, with particle size of 112.6 nm. However, the PR loaded CNG had a larger size (129.8 nm). A polydispersity index value below 0.3 was found, which indicates that CNG distribution was relatively homogeneous in size. Furthermore, CNG showed positive ZP for loaded and unloaded one. The entrapment efficiency achieved for CNG was found to be 62.5% and drug loading to be 38.4% for PR. This high entrapment and loading of PR in the prepared formulation is explained by chemical interaction between the drug and the CNG structure. The release of PR from CNG showed sustained release of 78% after 48 h, which could be attributed to drug diffusion and the swelling/degradation of the polymer (Keawchaoon and Yoksan, 2011). Table 1 represents these results.

Table 1 The composition and characterization of pravastatin loaded CS nanogels.

Parameters	PR loaded CS nanogels	Plain CS nanogels
CS/TPP ratio	3:1	3:1
Particle size (nm)	129.8 ± 10.5	112.6 ± 7.33
Polydispersity index	0.276 ± 0.04	0.211 ± 0.02
Zeta potential (mV)	25.10 ± 2.64	33.20 ± 3.22
Entrapment efficiency (%)	62.56 ± 1.19	–
Drug loading (%)	38.40 ± 0.26	–
Drug release 48 h (%)	78.12 ± 4.81	–

A SEM investigation was also performed to evaluate CNG morphology Fig. 1. The results showed that both unloaded CNG and PR loaded CNG had a roughly spherical shape. These results are in agreement with the results of previous studies reported that chitosan loaded nanocarriers have desirable physicochemical characters (Ravikumara and Madhusudhan, 2011). Moreover, FTIR and X-ray diffractograms were performed as a routine test, and FTIR results confirmed the absence of any chemical interaction between PR and chitosan. Moreover, X-ray diffractograms confirmed that PR was not crystalline form and was effectively entrapped in CNG (data not shown). This desirable formula was loaded into erythrocytes.

CNG have a good compatibility with erythrocytes, and CNG loaded erythrocytes may be served as a potential multifunctional delivery system (Fan et al., 2012). So, the hypotonic preswelling method was used to prepare PR–CSN loaded erythrocytes (PR–CSN–ER). This method is based on creation of transiently membrane pores, which permit the entrapment of drug into cells efficiently (Kostić et al., 2014). PR–CSN–ER were evaluated for their size, surface charge and shape, which improve the nanocarriers cellular uptake (Alexis et al., 2008; Sakhtianchi et al., 2013).

At positive zeta potential of the prepared CNG, there is considerable interaction with the negatively charged membrane of the erythrocyte. This behavior may result in higher cellular uptake (Bankapur et al., 2014; Ramasamy et al., 2014). Alexis et al., (2008), showed that the positively charged nanocarriers have higher cellular uptake compared to neutral or negatively charged one. Additionally, they were passively transported through the erythrocyte membrane (Treuel et al.,

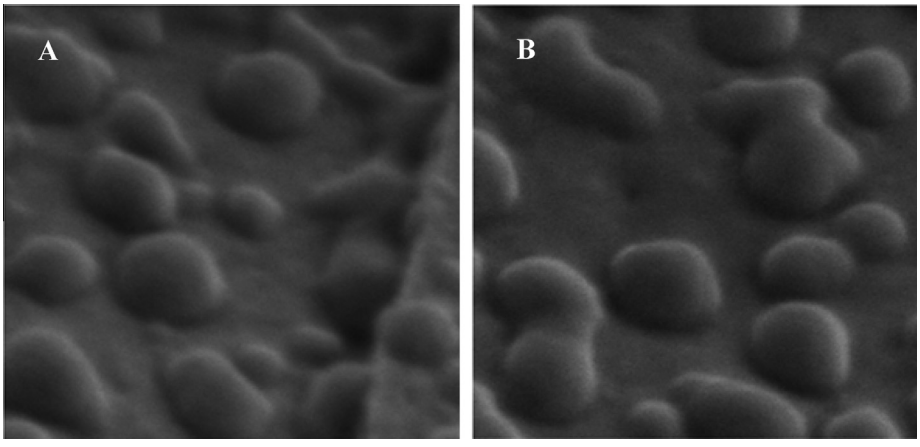

Figure 1 Scanning electron microscopic images of CNG (A) and PR–CNG(B).

2013). Table 2 shows percent of PR loading and cell recovery (CR) of PR-ER of PR–CNG–ER. These results are similar to those reported in the previous studies (Hamidi et al., 2011; Harisa et al., 2012; Harisa et al., 2014).

It was observed that zeta potential (ZP) of PR–CNG–ER and PR-PR is negative Table 2. This negative ZP of PR–CNG–ER prevents clumping and adhesion to capillary walls upon administration and avoids the interactions between erythrocytes and vascular cells (Diego et al., 2012). Furthermore, this maintains the stability of PR–CNG–ER and PR-PR.

In order to assess hemolysis percent of erythrocytes after loading, 0.4% NaCl solution was added to the samples of SH-ER, PR–CNG–ER and PR-ER. Table 2 shows that SH-ER have greater hemolysis compared to PR–CNG–ER and PR-ER. It has been reported chitosan has membrane-stabilizing properties (Anandan et al., 2013) and PR reduce oxidative stress (Liao and Laufs, 2005). These effects may be responsible for decreasing the percent of hemolysis in PR–CNG–ER and PR-ER compared with SH-ER.

Hematological parameters of erythrocytes were obtained after PR–CNG loading procedure and compared with those of SH-ER, PR-ER and unloaded erythrocytes (UER) Table 3. MCV, MCH and MCHC, were measured in order to evaluate the cell integrity after loading. MCV remained unchanged in all groups. However, other hematological indices were decreased in the loaded erythrocytes compared to unloaded cells. This may be attributed to hemoglobin loss during the loading procedure (Hamidi et al., 2011).

On the basis of cellular targeting, PS on the outer layer of erythrocyte was measured. PS is considered as a potential marker for rapid clearance by macrophages of spleen and liver cells (Schrijvers et al., 2007). In the present study, PS was showed on loaded erythrocytes as depicted in Fig. 2. It was obvious that PR–CNG–ER and PR-ER provoke PS exposure compared to unloaded erythrocytes. Similarly, Favretto et al., (2013), demonstrated that the preswelling technique causes an increase in exposure of PS. Additionally, incubation of erythrocytes in the presence of a hypotonic solution induced shift of PS to the external surface (Kostić et al., 2014). Exposure of PS on loaded erythrocytes may enhance liver targeting (Schrijvers et al., 2007; Alanazi et al., 2011; Bosman et al., 2011).

With respect to morphological characters of erythrocytes after loading, the erythrocyte exhibited deformation of the membrane. Fig. 3 represents the SEM images of control, PR–CNG–ER, PR-ER and SH-ER. It was shown that the loading process with and without the nanogel resulted in the formation of stomatocytes shape of erythrocytes compared to discocytes-biconcave shape of unloaded erythrocytes. These findings are in agreement with several studies, which reported that the loaded erythrocytes prepared by osmotic based methods have stomatocytes shape (Favretto et al., 2013). Likewise, Deuticke et al. (1973), demonstrated that stomatocytosis could be induced by amphipathic cations. The stomatocytes formation could be attributed to the changes in osmotic pressure in the presence of chitosan. Abnormal shape of erythrocytes became more trapped in the liver (Favretto et al., 2013).

PR is hydrophilic drug, so the rate of drug release is comparable to that of hemoglobin (see Table 2). Several mechanisms include passive diffusion, membrane associated carrier, and phagocytosis explain drug release from carrier erythrocytes (Hamidi et al., 2011). This indicates that cell lysis is essential for drug release and drug cannot be released by mere diffusion. PS exposure on erythrocytes membrane accelerates

Table 2 Percent of drug loading (DL), cell recovery (CR), hemoglobin release (HbR), pravastatin release (PR-R) of PR–CNG–ER and PR-ER as well as hemolysis percent (Hem), zeta potential (ZP), size distribution (SD) of UER, SH-ER, PR–CNG–ER and PR-ER.

Parameter	UER	SH-ER	PR–CNG–ER	PR-ER
DL (%)	–	–	36.85 ± 4.37	31.54 ± 3.62
CR (%)	–	58.21 ± 4.81	66.82 ± 5.42	60.32 ± 6.30
HbR48h (%)	–	–	90.13 ± 8.95	96.23 ± 7.52
PR-R 48h (%)	–	–	83.74 ± 7.62	93.34 ± 8.73
Hem. (%)	11.33 ± 0.92	35.32 ± 4. 21[a]	24.97 ± 3.21[a]	27.01 ± 2.82[a]
ZP (mV)	−14.82 ± 1.24	−11.34 ± 0.65	−10.83 ± 1.01[a]	−14.28 ± 1.05
SD (μm)	5.713 ± 0.54	5.254 ± 0.49	4.165 ± 0.3[a]	5.269 ± 0.56

Data represented as mean ± SD, (N = 6).
[a] Indicated when a significant change was observed.

Table 3 Hematological indices of unloaded erythrocytes (UER), sham-erythrocytes (SH-ER), PR–CNG-loaded erythrocytes (PR–CNG–ER) and pravastatin-loaded erythrocytes (PE-ER).

Parameter	UER	SH-ER	PR–CNG–ER	PR-ER
MCV (fl)	91.27 ± 2.12	96.63 ± 3.33	85.47 ± 9.13	86.37 ± 6.47
MCH (pg/cell)	30.37 ± 0.31	16.33 ± 1.92[a]	19.80 ± 2.15[a]	16.40 ± 1.30[a]
MCHC (g/dl)	33.43 ± 1.193	16.03 ± 2.39[a]	23.97 ± 0.95[a]	17.90 ± 1.40[a]

Data represented as mean ± SD, (N = 6).
[a] Indicated when a significant change was observed.

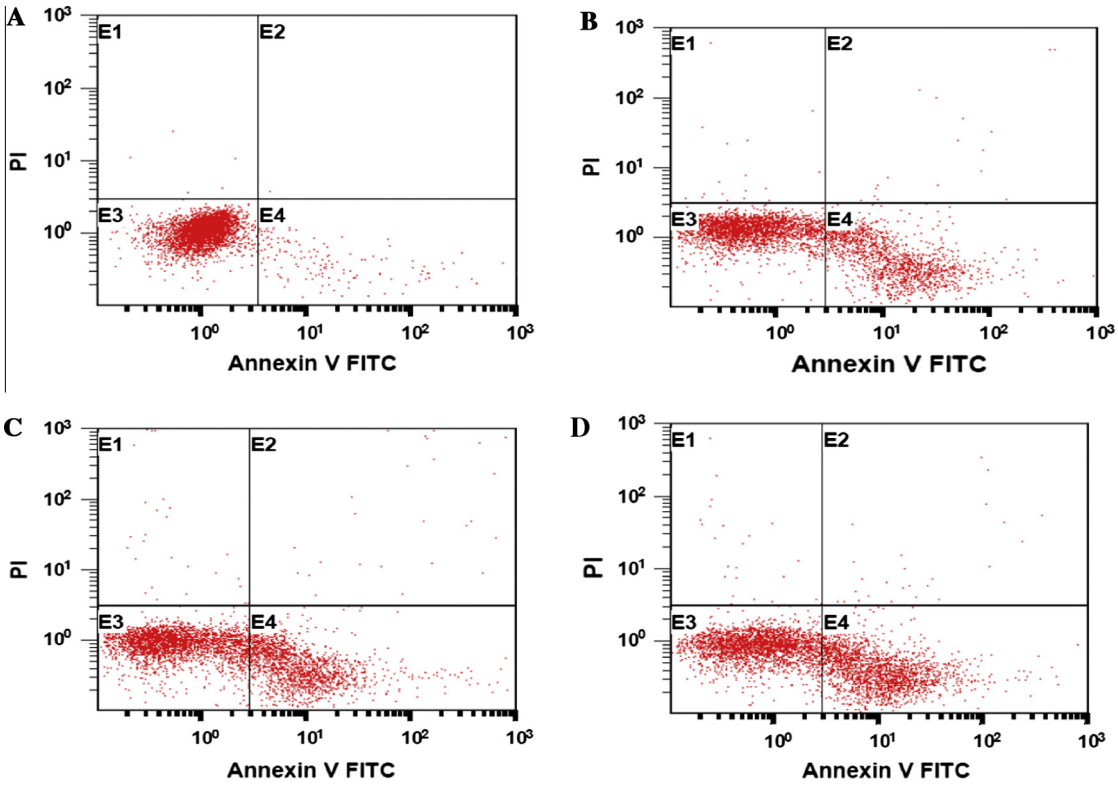

Figure 2 Phosphatidylserine (PS) exposure of UER (A), SH-ER (B), PR–CNG–ER (C) and PE-ER (D).

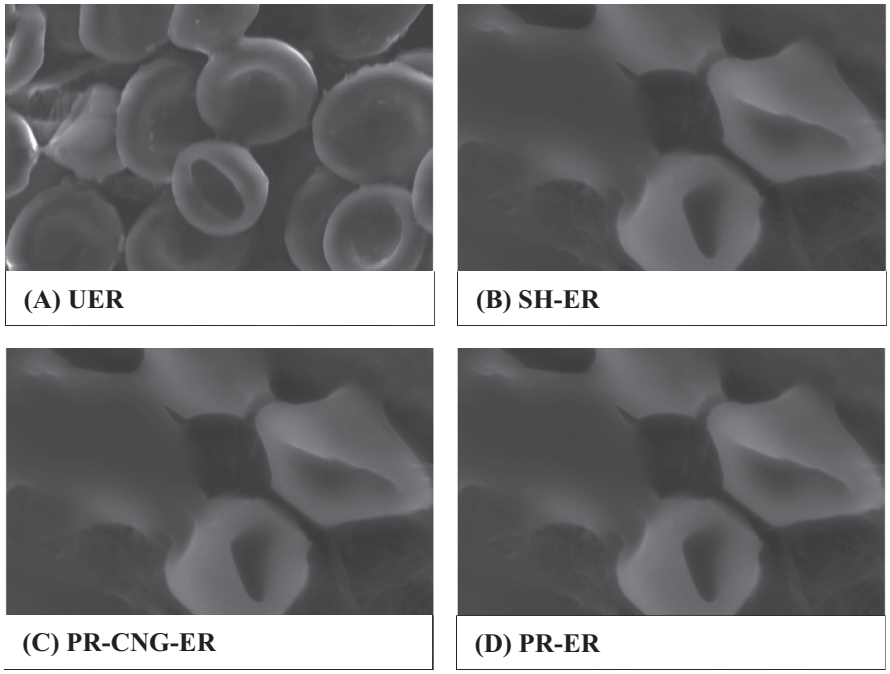

Figure 3 Scanning electron microscopy (SEM) images of UER, SH-ER, PR–CNG–ER and PE-ER. (A) Unloaded erythrocytes have discocytes shape. (B) Sham encapsulated stomatocytes shape of erythrocytes. (C) PR–CNG-loaded stomatocytes shape of erythrocytes, and (D) PR-loaded erythrocytes have stomatocytes. Magnification × 10.000.

phagocytosis and PR release from erythrocytes (Favretto et al., 2013; Kostić et al., 2014). These findings are in agreement with the results published previously (Hamidi et al., 2011; Hamidi et al., 2007). Moreover, the morphological changes and PS exposure on PR–CNG–ER may enhance their uptake by macrophages and accelerate PR release.

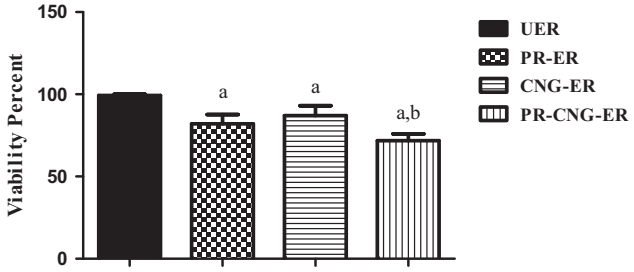

Figure 4 Effect of UER, PR-ER, CNG–ER, PR–CNG–ER on HepG2 cell line viability. Data represented as mean ± SD, ($N = 6$). a indicated significant decrease from unloaded erythrocytes, b indicated significant decrease from pravastatin loaded and chitosan nanogels-loaded erythrocytes, $P \leqslant 0.05$.

Additionally, nanocarriers preferentially accumulated in tumor cells by EPR effect (Noble et al., 2014; Upreti et al., 2013). Acidic environment of tumor tissues may promote drug release from nanogel (Arias, 2011).

The in vitro cytotoxicity of PR or PR–CNG loaded into erythrocytes was investigated by MTT assay using HepG2 cells as model HCC. Fig. 4 showed that the incubation of PR-ER, CNG–ER and PR–CNG–ER with HepG2 cells for 72 h resulted in the reduction of cell viability by 18%, 13% and 28%, respectively compared to unloaded erythrocytes. Shen et al., (2009) reported that the chitosan inhibits the proliferation of HepG2 cells. The cationic property of chitosan plays a significant role in the antitumor activity (Xia et al., 2011). Moreover, chitosan has the ability to disturb cell membrane, interfere with metabolism, induce apoptosis and inhibit tumor cells growth (Prabaharan, 2015). As well, Smith and Land, (2012) indicated that the antitumor effect of statin is due to the inhibition of cholesterol, which is considered as an essential membrane component and blocking protein lipidation (Smith and Land, 2012). The higher cytotoxicity of PR–CNG–ER could be due to the synergistic combination of chitosan and PR. Moreover, nanosize and positive charge of these carriers may enhance cellular uptake and promote more drug influx inside the cancer cell (Prabaharan, 2015).

4. Conclusion

This study concluded that CNG were successfully employed for the entrapment of PR. The investigated PR–CNG have nanosized particles, homogenous uniform distribution, higher entrapment and sustained release over 48 h. Moreover, PR–CNG loaded into erythrocytes had desirable loading parameters and release pattern of PR. The PR–CNG–ER exhibited stomatocytes shape, PS exposed, more fragile and higher cytotoxicity to HepG2 compared to unloaded erythrocytes. These results suggest that PR–CNG–ER can be used as promising delivery systems in liver cancer therapy. Further in vivo study is required to address this issue.

Acknowledgments

This project was supported by NSTIP strategic technologies programs, number (12-MED2563-02) in the Kingdom of Saudi Arabia.

References

Abdel-Hamid, M., Ibrahim, M.F., Harisa, G.I., Alanazi, F.K., 2012. Ultra performance liquid chromatography determination of pravastatin sodium in erythrocytes. Asian J. Chem. 24 (2), 584.

Alanazi, F.K., Harisa, Gel-D., Maqboul, A., Abdel-Hamid, M., Neau, S.H., Alsarra, I.A., 2011. Biochemically altered human erythrocytes as a carrier for targeted delivery of primaquine: an in vitro study. Arch. Pharm. Res. 34 (4), 563–571.

Alexis, F., Pridgen, E., Molnar, L.k., Farokhzad, O.C., 2008. Factors affecting the clearance and biodistribution of polymeric nanoparticles. Mole. Pharma. 5, 505–515.

Anandan, R., Ganesan, B., Obulesu, T., Mathew, S., Asha, K.K., Lakshmanan, P.T., Zynudheen, A.A., 2013. Antiaging effect of dietary chitosan supplementation on glutathione-dependent antioxidant system in young and aged rats. Cell Stress Chaperones. 18 (1), 121–125.

Arias, J.L., 2011. Drug targeting strategies in cancer treatment: an overview. Mini. Rev. Med. Chem. 11 (1), 1–17.

Bankapur, A., Barkur, S., Chidangil, S., Mathur, D., 2014. A micro-Raman study of live, single red blood cells (RBCs) treated with AgNO3 nanoparticles. PLoS One 9 (7), e103493.

Bhattarai, N., Gunn, J., Zhang, M., 2010. Chitosan-based hydrogels for controlled, localized drug delivery. Adv. Drug. Deliv. Rev. 62 (1), 83–99.

Bosman, G.J.C.G.M., Cluitmans, J.C.A., Groenen, Y.A.M., Were, J.M., Willekens, et al, 2011. Susceptibility to hyperosmotic stress-induced phosphatidylserine exposure increases during red blood cell storage. Transfusion 51, 1072–1078.

Deuticke, B., Kim, M., Zolinev, C., 1973. The influence of amphotericin-B on the permeability of mammalian erythrocytes to nonelectrolytes, anions and cations. Biochim. Biophys. Acta 318, 345–359.

Fan, W., Yan, W., Xu, Z., Ni, H., 2012. Erythrocytes load of low molecular weight chitosan nanoparticles as a potential vascular drug delivery system. Colloids Surf. B Biointerfaces 15 (95), 258–265.

Fang, R.H., Hu, C.M., Zhang, L., 2012. Nanoparticles disguised as red blood cells to evade the immune system. Expert Opin. Biol. Ther. 12 (4), 385–389.

Favretto, M.E., Cluitmans, J.C., Bosman, G.J., Brock, R., 2013. Human erythrocytes as drug carriers: loading efficiency and side effects of hypotonic dialysis, chlorpromazine treatment and fusion with liposomes. J. Control. Release 170 (3), 343–351, 28.

Graf, H., Jüngst, C., Straub, G., Dogan, S., Hoffmann, R.T., Jakobs, T., et al, 2008. Chemoembolization combined with pravastatin improves survival in patients with hepatocellular carcinoma. Digestion 78, 34–38.

Hamidi, M., Azadi, A., Rafiei, P., 2008. Hydrogel nanoparticles in drug delivery. Adv. Drug. Deliv. Rev. 60 (15), 1638–1649.

Hamidi, M., Rafiei, P., Azadi, A., Mohammadi-Samani, S., 2011. Encapsulation of valproate-loaded hydrogel nanoparticles in intact human erythrocytes: a novel nano-cell composite for drug delivery. J. Pharm. Sci. 100 (5), 1702–1711.

Hamidi, M., Zarei, N., Zarrin, A.H., Mohammadi-Samani, S., 2007. Preparation and in vitro characterization of carrier erythrocytes for vaccine delivery. Int. J. Pharm. 338 (1–2), 70–78.

Harisa, G.I., Ibrahim, M.F., Alanazi, F., Shazly, G.A., 2014. Engineering erythrocytes as a novel carrier for the targeted delivery of the anticancer drug paclitaxel. Saudi. Pharm. J. 22 (3), 223–230.

Harisa, G.I., Ibrahim, M.F., Alanazi, F.K., 2012. Erythrocyte-mediated delivery of pravastatin: in vitro study of effect of hypotonic lysis on biochemical parameters and loading efficiency. Arch. Pharm. Res. 35 (8), 1431–1439.

Hu, C.M., Zhang, L., Aryal, S., Cheung, C., Fang, R.H., Zhang, L., 2011. Erythrocyte membrane-camouflaged polymeric nanoparticles as a biomimetic delivery platform. Proc. Natl. Acad. Sci. U.S.A. 108 (27), 10980–10985.

Jiang, J.T., Xu, N., Zhang, X.Y., Wu, C.P., 2007. Lipids changes in liver cancer. J. Zhejiang Univ. Sci. B 8 (6), 398–409.

Keawchaoon, Yoksan, R., 2011. Preparation, characterization and in vitro release study of carvacrol-loaded chitosan nanoparticles. Colloids Surf., B: Biointer-faces 84, 163–171.

Kostić, I.T., Ilić, V.L.j., Đorđević, V.B., Bukara, K.M., Mojsilović, S.B., et al, 2014. Erythrocyte membranes from slaughterhouse blood as potential drug vehicles: isolation by gradual hypotonic hemolysis and biochemical and morphological characterization. Colloids Surf. B Biointerfaces 122, 250–259.

Kraus, A., Roth, H.P., Kirchgessner, M., 1997. Supplementation with vitamin C, vitamin E or beta-carotene influences osmotic fragility and oxidative damage of erythrocytes of zinc-deficient rats. J. Nutr. 127, 1290–1296.

Liao, J., Laufs, K.U., 2005. Pleiotropic effects of statins. Annu. Rev. Pharmacol. Toxicol. 45, 89–118.

Menter, D.G., Ramsauer, V.P., Harirforoosh, S., Chakraborty, K., Yang, P., His, L., Newman, R.A., Krishnan, K., 2011. Differential effects of pravastatin and simvastatin on the growth of tumor cells from different organ sites. PLoS One 6 (12), e28813.

Montori, V.M., Brito, J.P., Ting, H.H., 2014. Patient-centered and practical application of new high cholesterol guidelines to prevent cardiovascular disease. JAMA 311, 465–466.

Muzykantov, V.R., 2010. Drug delivery by red blood cells: vascular carriers designed by mother nature. Expert Opin. Drug. Deliv. 7 (4), 403–427.

Noble, G.T., Stefanick, J.F., Ashley, J.D., Kiziltepe, T., Bilgicer, B., 2014. Ligand-targeted liposome design: challenges and fundamental considerations. Trends Biotechnol. 32 (1), 32–45.

Prabaharan, M., 2015. Chitosan-based nanoparticles for tumor-targeted drug delivery. Int. J. Biol. Macromol. 72C, 1313–1322.

Ramasamy, T., Tran, T.H., Cho, H.J., Kim, J.H., Kim, Y.I., Jeon, J.Y., Choi, H.G., et al, 2014. Chitosan-based polyelectrolyte complexes as potential nanoparticulate carriers: physicochemical and biological characterization. Pharm. Res. 31 (5), 1302–1314.

Ravikumara, N.R., Madhusudhan, B., 2011. Chitosan nanoparticles for tamoxifen delivery and cytotoxicity to MCF-7 and Vero cells. Pure Appl. Chem. 83 (11), 2027–2040.

Reijnders, L., 2006. Cleaner nanotechnology and hazard reduction of manufactured nanoparticles. J. Clean. Prod. 14, 124–133.

Sakhtianchi, R., Minchin, R.F., Lee, K.B., Alkilany, A.M., Serpooshan, V., Mahmoudi, M., 2013. Exocytosis of nanoparticles from cells: role in cellular retention and toxicity. Adv. Colloid Interface Sci. 201–202, 18–29.

Schrijvers, D.M., De Meyer, G.R., Herman, A.G., Martinet, W., 2007. Phagocytosis in atherosclerosis: molecular mechanisms and implications for plaque progression and stability. Cardiovasc. Res. 73 (3), 470–480.

Shen, K.T., Chen, M.H., Chan, H.Y., Jeng, J.H., Wang, Y.J., 2009. Inhibitory effects of chitooligosaccharides on tumor growth and metastasis. Food Chem. Toxicol. 47 (8), 1864–1871.

Silva, Diego C.N., Jovino, Cauêh N., Silva1, Carlos A.L., Heloise, et al, 2012. Optical tweezers as a new biomedical tool to measure zeta potential of stored red blood cells. PLoS ONE 7 (2), e31778.

Smith, B., Land, H., 2012. Anticancer activity of the cholesterol exporter ABCA1 gene. Cell Rep. 2 (3), 580–590.

Treuel, L., Jiang, X., Nienhaus, G.U., 2013. New views on cellular uptake and trafficking of manufactured nanoparticles. J. R. Soc. Interface 10 (82), 20120939.

Upreti, M., Jyoti, A., Sethi, P., 2013. Tumor microenvironment and nanotherapeutics. Trans. Cancer Res. 2 (4), 309–319.

Xia, W., Liu, P.c., Zhang, J., Chen, J., 2011. Biological activities of chitosan and chitooligosaccharides. Food Hydrocoll. 25, 170–179.

Yew, N.S., Dufour, E., Przybylska, M., Putelat, J., Crawley, C., et al, 2013. Erythrocytes encapsulated with phenylalanine hydroxylase exhibit improved pharmacokinetics and lowered plasma phenylalanine levels in normal mice. Mol. Genet. Metab. 109 (4), 339–344.

Zhang, F., Du, G., 2012. Dysregulated lipid metabolism in cancer. World J. Biol. Chem. 3 (8), 167–174, 26.